



Assessment of the impact of impervious surface increase on urban heat island and vegetation by remote sensing and statistical analysis: the case of Türkiye/Niğde city center (2013-2024)

Münevver Gizem Gümüş^{*1} , Kutalmış Gümüş¹ 

¹ Niğde Omer Halisdemir University, Faculty of Engineering, Department of Surveying Engineering, Niğde, Türkiye; gizemkisaaga@ohu.edu.tr; kgumus@ohu.edu.tr



Article History:

Received: 23 March 2025

Revised: 15 April 2025

Accepted: 30 April 2025

Published: 30 June 2025



Copyright: © 2025 by the authors.

This article is an open access article distributed under terms and conditions of the Creative Commons Attribution (CC BY-SA) license. <https://creativecommons.org/licenses/by-sa/4.0/>

Abstract: The expansion of impervious surfaces, reduction of vegetation cover, and heat-retaining properties of artificial materials intensify the Urban Heat Island (UHI) effect, leading to higher surface temperatures in urban areas compared to rural surroundings. This phenomenon increases energy demand, interacts with climate change, and negatively impacts public health. This study investigates the spatial and temporal changes in vegetation, impervious surface density, and land surface temperature (LST) in Niğde, Türkiye, between 2013 and 2024. NDVI (Normalized Difference Vegetation Index), NDBI (Normalized Difference Built-up Index), and LST were derived from Landsat 8 OLI/TIRS satellite imagery and analyzed using Google Earth Engine (GEE) and ArcGIS 10.8. Index values were extracted from 500 randomly distributed points. Data normality was assessed using Kolmogorov-Smirnov and Shapiro-Wilk tests. Paired sample t-tests and Wilcoxon signed-rank tests were used to evaluate temporal differences, while Pearson, Spearman's rho, and Kendall's tau-b correlation coefficients were used to determine the level of relationship between variables. Results show no significant change in NDVI ($p > 0.05$), but statistically significant increases in both NDBI and LST ($p < 0.05$). A strong negative correlation was observed between NDVI and NDBI ($r = -0.91$), and a positive correlation between NDBI and LST ($r = 0.39$). Between 2013 and 2024, impervious surfaces expanded by 59.63% (from 14.02 km² to 22.38 km²), while dense vegetation areas declined by 50%. These findings confirm that urbanization has led to vegetation loss and increased surface temperatures. The study offers valuable insights into the UHI effect using remote sensing and statistical analysis and contributes to sustainable urban planning and climate adaptation strategies.

Keywords: Google earth engine; LST; NDBI; NDVI; spatial analysis; impervious surface

Citation: Gümüş, M. G., Gümüş, K. (2025). Assessment of the impact of impervious surface increase on urban heat island and vegetation by remote sensing and statistical analysis: the case of Türkiye/Niğde city center (2013-2024). *Turk. J. Remote Sens.*, 7(1), 69-90. <https://doi.org/10.51489/tuzal.1663695>

1. Introduction

Urbanization is a rapidly increasing process worldwide, and land use changes and the replacement of natural surfaces with artificial surfaces have important consequences for urban climate and environmental sustainability. The increase in impervious surfaces (concrete, asphalt, etc.) in urban areas, the decrease in vegetation cover, and the density of heat-absorbing artificial surfaces reveal the UHI effect. UHI causes urban areas to have higher surface temperatures than the surrounding rural areas, with direct impacts on climate change, energy consumption, and public health (Voogt & Oke, 2003). According to the projections of the United Nations, the proportion of urban population is gradually increasing worldwide and is estimated to reach 66% by 2050, up from 54% in 2014. In Turkey, the urban population was 73% in 2015 and is projected to reach 84% by 2050 (UNPD, 2015). This rapid urbanization process leads to significant changes in land use and makes the urban heat island effect more pronounced with the expansion of impermeable surfaces.

The study of surface temperature changes in urban areas can be carried out using remote sensing techniques and geographic information systems (GIS) (Bauer et al., 2004). Indicators such as LST, NDVI, and NDBI are important parameters to study the impact of

urbanization on surface temperatures (Weng et al., 2004; Zhang et al., 2009). NDVI helps to understand the thermal properties of natural surfaces by determining the density of vegetation cover, while NDBI is a critical index used to describe the density of urban development. Studies have revealed that the relationship between NDVI and LST is generally weakly correlated in a negative direction, but there is a strong positive correlation between NDBI and LST. Yuan & Bauer (2007) analyzed the UHI effect on impervious surface areas and its relationship with LST. In this study using Landsat satellite imagery, a negative correlation was found between NDVI and LST, while a strong positive correlation was found between NDBI and LST. The study shows that the increase in impervious surfaces is an important indicator in understanding urban temperature dynamics. Shrestha et al. (2021) analyzed the impervious surface growth and growth trends of Lahore city in 2015 and 2021 using data from Sentinel-1, Sentinel-2, and Random Forest classifier. The study showed that this data fusion is a reliable method for impervious surface mapping as an indicator of environmental quality. Sarkar Chaudhuri et al. (2017) examined the impact of urban growth on water resources and the hydrological cycle in India and showed that the increase in ISA has negative impacts on urban ecosystems and that remote sensing techniques can successfully map the spatial changes of impervious surfaces.

Guha et al. (2021) examined the relationship between LST and NDBI over four seasons between 1991 and 2019 in Raipur, India. 64 Landsat images were analyzed, and seasonal correlations were evaluated. The highest positive correlation between LST and NDBI was found in summer (0.72) and the lowest in winter (0.57). It was emphasized that construction increases surface temperatures. Chen et al. (2013) analyzed the relationship between NDVI, NDBI, and LST with Landsat ETM+ data covering four seasons in Wuhan City. Strong positive correlations (0.639-0.807) were found between NDBI and LST, while weaker negative correlations (-0.568 to -0.242) were found between NDVI and LST. It was concluded that NDBI reflects the urban heat island effect. Alademomi et al. (2022) examined the relationship between LST, NDVI, and NDBI in the context of LULC change in Lagos Metropolis over the period 2002-2019. It was determined that NDBI and LST values increased together in areas with increased structuring, and there was a negative relationship between NDVI and LST. Strong agreement was observed between land cover transformations and spectral indices. Keerthi Naidu & Chundeli (2023) analyzed the impact of LULC changes on LST with NDVI and NDBI between 2003 and 2021 in Bengaluru city. It was found that green areas decreased by 50% and LST increased from 26 °C to 29 °C. NDVI-LST was negatively correlated, and NDBI-LST was positively correlated. Zhang et al. (2009) analyzed the relationship between impervious surfaces and LST at different spatial resolutions (30-960 m). In the study, a strong negative correlation was found between NDVI and LST, while a positive correlation was shown between ISA and LST. Parekh et al. (2021) used Landsat 8 imagery to detect impervious surfaces with deep learning methods and demonstrated the effect of ISA on UHI. In the study, it was concluded that LST is directly related to ISA and shows an inversely proportional change with NDVI. Kesikoğlu et al. (2021) classified impervious surfaces in the city center of Kayseri using Landsat satellite images using the Impervious Surface Index (NDAISI) and Support Vector Machines (SVM) methods and associated these classification results with LST. In the study, it was determined that by using the NDAISI and SVM methods together, impervious surfaces and soil areas were separated more accurately, and their effects on surface temperatures were evaluated more sensitively. In the study conducted by Jamei et al. (2022), the effect of land use/cover change in Melbourne on LST was analyzed. In the study conducted using the GEE platform, it was determined that LST increased by 5.1°C between 2001 and 2018, and this increase was observed most in built-up areas with high NDBI. Liu et al. (2023) analyzed the spatial and temporal changes in impervious surface areas in the Yellow River Delta using Sentinel-1 and Sentinel-2 data. The study conducted with the

GEE and random forest algorithm revealed that ISA decreased between 2018 and 2022, but there was no significant change in the spatial distribution pattern. In the study of Fıçıcı (2024), the urban sprawl on the Trabzon coastline was analyzed using the Global Human Settlement Layer (GHSL) and GEE. In the study, it was determined that the density of construction on the coastline increased and tended to expand towards the inner parts. Most of the studies on the urban heat island effect have focused on large-scale cities and densely urbanized regions. However, the lack of detailed studies addressing the long-term spatial and temporal changes of this effect in medium-sized cities is striking. In addition, although the relationship between urban construction and vegetation changes with surface temperatures has been examined in a general framework, studies using statistical methods together with GEE-based analyses are quite limited.

In this context, this study aims to contribute to the scientific literature by analyzing the relationship between impermeable surface increase, vegetation change, and surface temperature in Niğde city center between 2013 and 2024 with multiple remote sensing indices (NDVI, NDBI, LST). In this context, relevant indices were derived using Landsat 8 Operational Land Imager (OLI) & Thermal Infrared Sensor (TIRS) satellite images on the GEE platform and transferred to ArcGIS 10.8 software for spatial analysis. In addition, statistical relationships between the index values obtained in different periods were evaluated with a paired sample t-test and correlation analysis, and the role of urban development on the heat island effect was examined in detail. The findings are expected to make significant contributions to sustainable urban planning, adaptation to climate change, and environmental management strategies. The study provides a comprehensive assessment aimed at understanding the spatial and temporal changes in urban temperature dynamics with remote sensing and GIS-based analyses.

2. Materials and Methods

In this study, urban growth, surface temperature changes, and land use dynamics occurring in Niğde city center between 2013 and 2024 were examined. The findings were evaluated based on NDVI, NDBI, and LST analyses, and spatial and temporal changes were discussed comparatively. For 2013 and 2024 data, various analyses were applied to determine the statistical differences and relationships between variables. Normal distribution was evaluated with Kolmogorov-Smirnov and Shapiro-Wilk tests, and linear relationships were examined with Pearson, Kendall's tau-b, and Spearman's rho correlation coefficients. A paired sample t-test and Wilcoxon signed-rank test were used to determine the change between the two years. The study area, the stages of satellite image evaluation, the derived NDVI, NDBI, and LST indices, and the statistical analysis methods applied are mentioned in this section. All statistical analyses were performed using SPSS software. Comparisons were made between parametric and nonparametric tests, and the results of both tests were evaluated together. The results obtained were used to understand the changes in NDVI, NDBI, and LST indices over time and to examine their relationship with environmental factors. The combined use of parametric and nonparametric tests increased the statistical reliability of the changes between the indices and enabled more robust inferences to be made. The methodological flow of the study is shown in Figure 1.

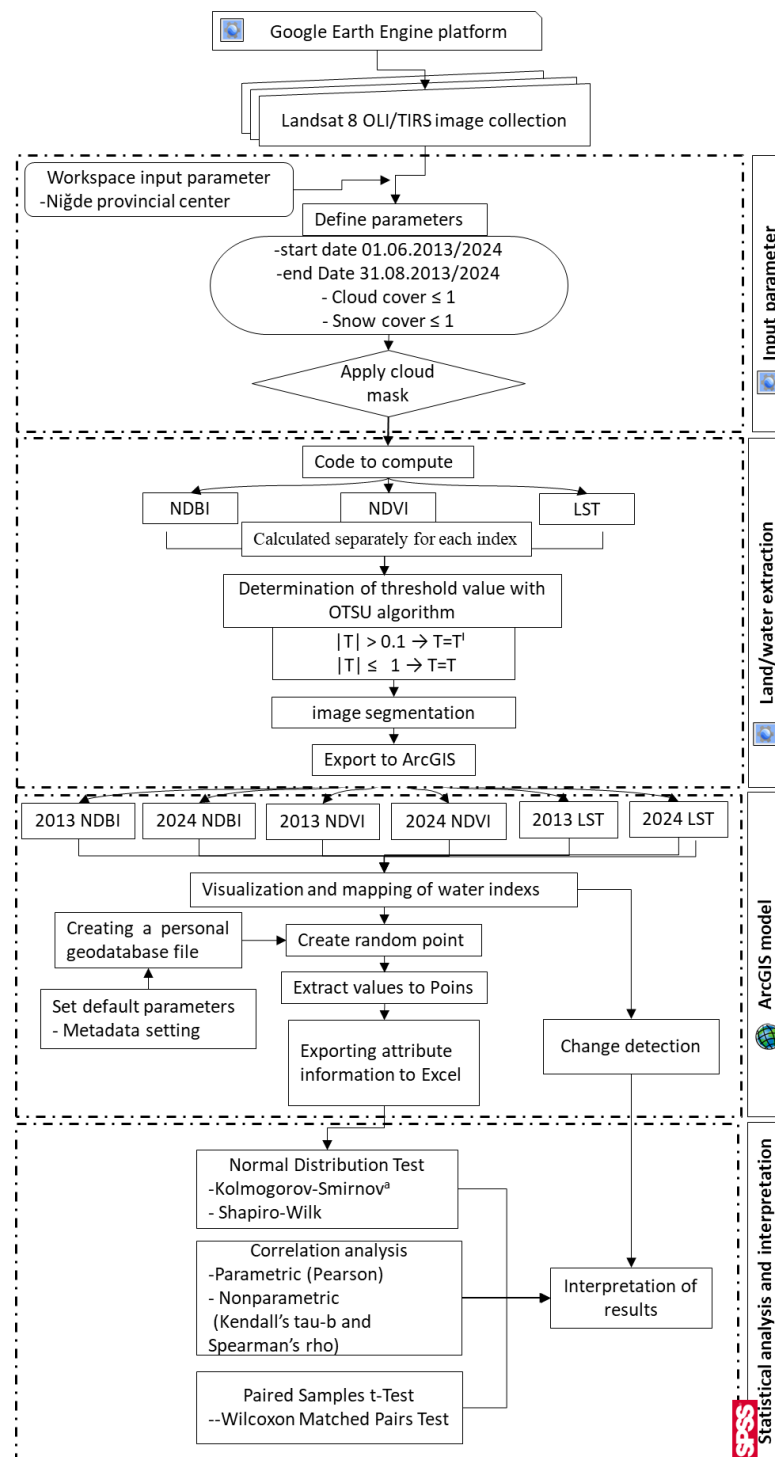


Figure 1. Workflow diagram of the study

2.1. Study area

This study was conducted in the city center of Niğde, located in the Central Anatolia Region of Turkey (Figure 2). Located between 37°58' north latitude and 34°41' east longitude, the city has an altitude of approximately 1,229 meters. Niğde is surrounded by Nevşehir and Kayseri to the east, Aksaray to the west, and Adana and Mersin to the south. The city has a continental climate with hot and dry summers and cold and snowy winters. The average annual temperature varies between 11 and 12°C, and while the temperature can exceed 35°C in summer, it can drop to -10°C in winter. Climatic dynamics have a determining

effect on urbanization processes and seasonal and temporal changes in surface temperatures (KTB, 2014).

Niğde is a medium-sized city with a population of approximately 230,000 by 2023 (TÜİK, 2025). In recent years, the development of industrial areas, the increase in new housing projects, and the expansion of transportation infrastructure have led to the spread of impervious surfaces in the city center and a decrease in natural land cover. In Niğde, which traditionally has plains suitable for agriculture and natural green areas, significant losses are occurring in these areas due to rapidly increasing construction. The decrease in vegetation cover and the increase in impermeable surfaces cause the surface temperatures in the city center to rise, making the UHI effect increasingly evident.

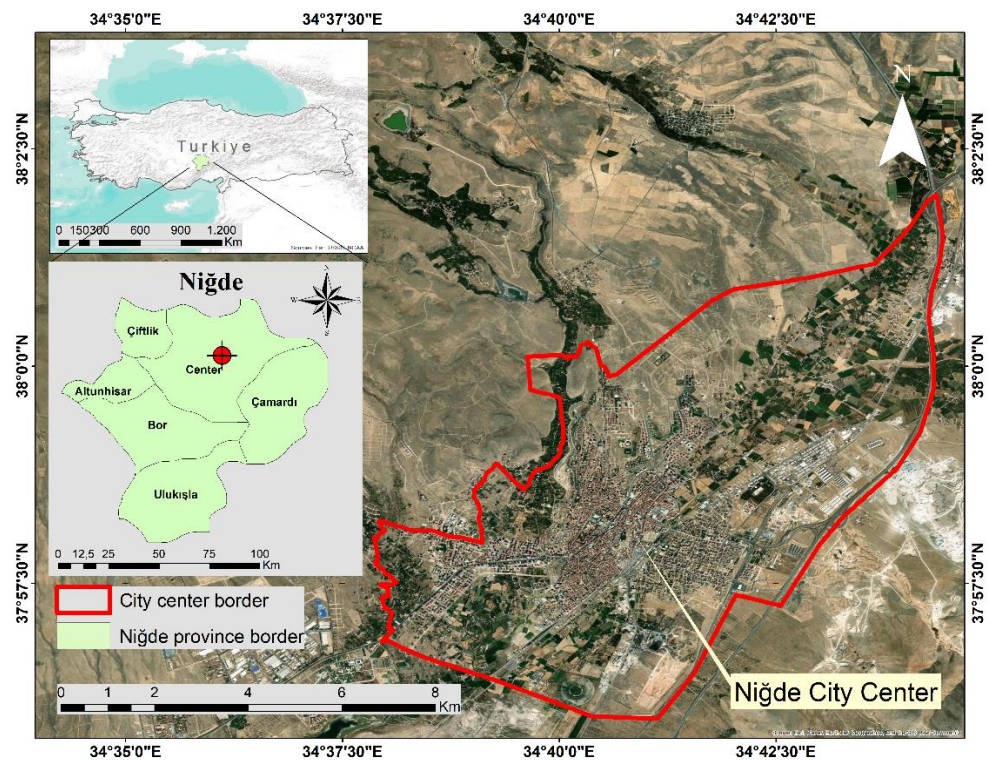


Figure 2. Geographical location of the study area: Niğde city center, Türkiye

2.2. Characteristics and selection of satellite images

In this study, Landsat 8 OLI/TIRS satellite imagery was used to analyze the urban density change, surface temperature changes, and UHI effect in Niğde city center. Landsat 8 was launched by the US Geological Survey (USGS) and NASA in 2013 and provides multispectral imagery with a spatial resolution of 30 meters. Thermal infrared data have a spatial resolution of 100 meters and are used to calculate surface temperature (USGS, 2013).

Landsat 8 OLI/TIRS images of the summer season (June-July-August) for the years 2013 and 2024 were preferred in the study. The summer months offer an ideal time interval for analysis, as they are the periods when vegetation density and surface temperatures are the most prominent and allow the spatial distribution of urban density to be observed in the best way (Lambin & Ehrlich, 1996). The satellite imagery used in the study was Landsat 8 OLI/TIRS, which was preferred because it has spectral and thermal bands suitable for NDVI, NDBI, and LST calculations and is open access. The technical specifications of the satellite imagery used are presented in Table 1.

Table 1. Technical specifications of the satellite images used (USGS, 2013)

Satellite & Sensor	Date	Spatial Resolution	Spectral Bands	Usage Purpose	Temporal Resolution	Source
Landsat 8 OLI Level 2	2013, 2024 (June, July, August)	30 m (visible and NIR), 15 m (panchromatic)	Band 4 (Red), Band 5 (NIR)	NDVI	16 Days	GEE, ee.ImageCollection('LANDSAT/LC08/C02/T1_L2')
Landsat 8 TIRS Level 2	2013, 2024 (June, July, August)	100 m (Thermal)	Band 10 (Thermal Infrared 1)	LST	16 Days	GEE, ee.ImageCollection('LANDSAT/LC08/C02/T1_L2')
Landsat 8 OLI Level 2	2013, 2024 (June, July, August)	30 m	Band 6 (SWIR 1), Band 5 (NIR)	NDBI	16 Days	GEE, ee.ImageCollection('LANDSAT/LC08/C02/T1_L2')

2.3. Normalized difference vegetation index (NDVI)

It is one of the most common spectral indices used to determine the density and health of vegetation. It was developed to assess the photosynthetic activity and water content of plants in remote sensing images and is a critical indicator for analyzing spatial and temporal changes in vegetation cover. NDVI is calculated based on the difference in reflectance between the red and near-infrared (NIR) bands of the electromagnetic spectrum. Since healthy vegetation shows high reflectance in the NIR band and low reflectance in the red band, NDVI values provide important information about the density of vegetation (Gümüş & Durduran, 2023). NDVI is calculated by the mathematical formula presented in equation 1:

$$NDVI = \frac{(NIR - Red)}{(NIR + Red)} \quad (1)$$

Where, *NIR* (Near Infrared): Landsat 8 OLI Band 5 (0.85 - 0.88 µm), *Red*: Landsat 8 OLI Band 4 (0.64 - 0.67 µm).

The NDVI value varies between -1 and +1. Values close to +1 indicate dense and healthy vegetation cover. Values close to 0 represent bare soil or areas with little vegetation cover. Negative values (-1 to 0) refer to reflective surfaces such as water surfaces, snow, and clouds (Hatfield et al., 1985).

2.4. Normalized difference built-up Index (NDBI)

It is a remote sensing index used to determine the density of construction and impervious surfaces in urban areas (Ünver & Başkaya, 2024). Since concrete, asphalt, and other artificial surfaces show different reflectivity properties in the near infrared (NIR) and shortwave infrared (SWIR) bands, built-up areas can be effectively detected using these bands.

NDBI is calculated by the mathematical formula presented in equation 2:

$$NDBI = \frac{(SWIR - NIR)}{(SWIR + NIR)} \quad (2)$$

Here: *SWIR* (Short Wave Infrared): Refers to Landsat 8 OLI Band 6 (1.57 - 1.65 µm).

The NDBI value varies between -1 and +1. Values close to +1 indicate areas of high built density. Values close to 0 represent open areas or areas of low built density. Negative values (-1 to 0) refer to impervious surfaces such as vegetation, water surfaces, or agricultural fields.

2.5. Land surface temperature (LST)

It is the temperature value calculated based on the thermal radiation emitted by a surface (Tonyaloğlu, 2019). LST is calculated by taking into account atmospheric and surface

properties with remote sensing techniques and is used as a basic parameter in urban heat island (UHI) studies. Unlike air temperature, LST depends on the capacity of the surface to absorb and re-radiate heat energy from the sun (Gümüş & Durduran, 2024).

Landsat 8 TIRS (Thermal Infrared Sensor) Band 10 was used to calculate LST, and the calculation consisted of the following three basic steps (Chen et al., 2002):

a) Conversion of pixel values (DN) to spectral radiances: The DN values obtained from the thermal bands are converted to radiances using the calibration coefficients (K_1 and K_2) for Landsat 8 (equation 3):

$$L_\lambda = M_L \times Q_{cal} + A_L - O_i \quad (3)$$

Here, L_λ : Spectral radiance ($W/m^2 \cdot sr \cdot \mu m$), M_L : Multiplicative rescaling factor for Band 10, Q_{cal} : Pixel value (DN), A_L : Additive rescaling factor for Band 10, and O_i : Band 10 correction factor

b) Conversion of Radiance to Brightness Temperature (BT): The brightness temperature (BT) is calculated using the following equation (equation 4):

$$BT = \frac{K_2}{\ln\left(\frac{K_1}{L_\lambda} + 1\right)} - 273.15 \quad (4)$$

Where BT : Brightness temperature ($^{\circ}C$), K_1 and K_2 : Thermal conversion coefficients determined for Landsat 8 TIRS Band 10, L_λ : Refers to the spectral radiance value.

c) Calculation of Emissivity Value: In the LST calculation, the emissive capacity of the surface is calculated using NDVI to determine the diffusion coefficient (equation 5-6):

$$P_v = ((NDVI_v - NDVI_s)/(NDVI - NDVI_s))^2 BT = \frac{K_2}{\ln\left(\frac{K_1}{L_\lambda} + 1\right)} - 273.15 \quad (5)$$

Where, P_v : Vegetation ratio, $NDVI_s$: NDVI threshold for soil (minimum value), $NDVI_v$: NDVI threshold for vegetation (maximum value) (Sobrino et al., 2004).

$$\varepsilon = 0.004 * P_v + 0.986 \quad (6)$$

Here, ε refers to the ground surface diffusivity value.

d) Calculation of Land Surface Temperature values: In the last step, land surface temperature is obtained by applying emissivity correction. In the study, it was calculated separately for 2013 and 2025 according to the ground surface diffusivity value (equation 7).

$$LST = BT / \{1 + \lambda(BT/\rho) \ln \varepsilon\} \quad (7)$$

Where, LST : Land surface temperature ($^{\circ}C$), BT : Brightness temperature ($^{\circ}C$), λ : Wavelength of emitted radiation ($11.5 \mu m$), ε : Emissivity (Akyürek, 2020).

2.6. Using google earth engine (GEE) and data processing

In this study, the GEE platform was used to calculate and spatially analyze NDVI, NDBI, and LST indices derived from Landsat 8 OLI/TIRS satellite imagery. GEE is a cloud-based geographic computing environment that enables fast and efficient analysis of large volumes of satellite data (Gorelick, 2013). Thanks to these features, NDVI, NDBI, and LST calculations; time series analysis; and spatial patterns were determined. Landsat 8 OLI/TIRS satellite images used in the study were obtained from the USGS source from the GEE data archive (USGS, 2013). The analyses were conducted on composite images of the summer season (June-July-August) of 2013 and 2024. Although the NDVI gives the best results in May, summer imagery was used due to the high cloudiness of the imagery. The summer season was preferred for the analysis because it is the period when surface temperatures reach the highest values. In the pre-processing process, satellite images covering the city center of

Niğde were selected. Atmospheric effects were minimized by applying cloud masking. The images were processed and combined for spatial and temporal analysis. The codes developed for the analyses conducted in this study are provided in Appendix A.

2.7. Normal distribution tests

In this study, the conformity of NDVI, NDBI, and LST index values of 2013 and 2024 to normal distribution was evaluated using Kolmogorov-Smirnov (K-S) and Shapiro-Wilk (S-W) tests. Normal distribution is a type of distribution widely used in statistical analysis and constitutes the basic assumption of many statistical tests (Gümü, 2024). The Kolmogorov-Smirnov test is a nonparametric test used in large data sets ($n > 50$) and assesses normality by measuring the difference between the observed distribution and the theoretical normal distribution. However, since it can consider even small deviations significant in large samples, it is recommended to supplement the results with visual analysis such as histograms and Q-Q plots. The Shapiro-Wilk test is a more sensitive test for small and medium-sized data sets ($n \leq 50$) and assesses the expectation of a normal distribution using the ordered observation values in the data set. It is more powerful than the K-S test, especially in detecting skewness and outliers (Razali & Wah, 2011). If the p-value of both tests is less than 0.05, the assumption of normal distribution is rejected, and it is recommended to use nonparametric tests instead of parametric tests. In general, the Shapiro-Wilk test is more reliable for small samples, while for large data sets the Kolmogorov-Smirnov test should be used as a reference and supported by graphical methods (Genceli, 2007).

2.8. Paired sample t tests

When it is accepted that the data are normally distributed and meet the valid assumptions of parametric testing, the parametric paired sample t-test is used. This test is suitable for assessing whether the mean differences between two dependent measures on the same group are statistically significant (Okoye & Hosseini, 2024). For each index (NDVI, NDBI, and LST), the differences between data from 2013 and 2024 were tested in this study. This test is based on H_0 (null hypothesis) and H_1 (alternative hypothesis). According to hypothesis H_0 , the mean difference of the indices between 2013 and 2024 is zero, meaning that the difference between the two years is not statistically significant. In contrast, hypothesis H_1 suggests that the mean difference of the indices is different from zero and the change between the two years is statistically significant. In the analyses conducted in line with these hypotheses, if the p-value is less than 0.05, H_0 is rejected, and the difference between the two years is accepted as significant. Otherwise, H_0 is accepted, and it is concluded that the change is not statistically significant (Manfei et al., 2017). In cases where the data were not normally distributed or the assumptions required by parametric testing were not met, the nonparametric Wilcoxon Paired Two Sample Test was used. This test is specifically based on rank-based analysis of data and tests whether there is a significant difference by using the ranks of the differences between two dependent samples (Blair & Higgins, 1985). This test is especially preferred when the data do not follow a normal distribution or contain outliers. In the analysis process, the differences between the indices for the years 2013 and 2024 are ranked, and it is evaluated whether the ranked differences are statistically significant. The Z value and p value obtained as a result of the test are used to determine whether the change between the indices is significant. The test is based on two hypotheses. Hypothesis H_0 states that the difference in the ranking of the indices between 2013 and 2024 is zero, meaning that the difference between the two years is not statistically significant. On the other hand, hypothesis H_1 states that the ranking difference is different from zero and the change between the two years is significant. If the p-value is less than 0.05,

the H_0 hypothesis is rejected, and the difference between the two periods is statistically significant. However, if the p-value is greater than 0.05, the hypothesis H_0 is accepted, and it is concluded that there is no significant change in the indices.

2.9. Correlation analysis

Correlation analysis is a statistical method that determines the strength and direction of the linear relationship between two variables (İnan, 2009). In this study, Pearson's correlation coefficient was used as a parametric correlation method, and Kendall's tau-b and Spearman's rho coefficients were used as non-parametric methods to evaluate the relationships between NDVI, NDBI, and LST indices for the years 2013 and 2024. Pearson's correlation coefficient (r) is an indicator that measures the direction and strength of the linear relationship between two continuous variables. The r value varies between -1 and 1 and determines the strength of the relationship. A positive r value ($r > 0$) indicates that there is a linear relationship between the variables, i.e., as one increases, the other increases. A negative r value ($r < 0$) indicates an inverse relationship; as one variable increases, the other decreases. When $r = 0$, there is no linear relationship between the variables. Pearson correlation is a parametric method that works under the assumption of normal distribution, and its reliability decreases when the data are not normally distributed (Kale & Erişmiş, 2024). Therefore, nonparametric methods should be used when the assumption of normal distribution is not met.

Spearman's rho (ρ) correlation is a nonparametric method based on the rankings of the data and can identify non-linear but monotonic relationships (Kılıç, 2022). It can be applied without depending on the normal distribution and can give more reliable results than Pearson correlation, especially in data sets where outliers are effective. Spearman's coefficient also varies between -1 and 1. Kendall's tau-b (τ -b) correlation is another nonparametric test that measures the direction and strength of the relationship between two ordinal variables. It can give stronger results than Spearman's correlation, especially for small samples. By measuring the consistency between the ranks of the variables, it identifies monotonic relationships and reduces the effect of outliers. Kendall's tau-b coefficient also ranges between -1 and 1, but its absolute value may be lower than Spearman's coefficient. In this study, parametric and non-parametric correlation methods were used together to analyze the relationships between NDVI, NDBI, and LST more comprehensively.

3. Results

In this study, the results obtained from the indices derived from satellite images and statistical analyses applied to examine the urban growth, surface temperature changes, and land use dynamics occurring in Niğde city center between 2013 and 2024 are given in this section. Important results to understand the impact of the urbanization process on the vegetation cover, the increase in the rate of construction, and the change in surface temperatures in Niğde city center are presented in this section.

In this study, the calculation and spatial analysis of NDVI, NDBI, and LST indices derived from Landsat 8 OLI/TIRS level 2 satellite images with the GEE platform were performed. 2013 and 2024 summer season (June-July-August) satellite images were analyzed; images of Niğde city center were selected in the pre-processing process, and appropriate atmospheric corrections were applied to enhance the accuracy of the data. The results indicate significant variations in vegetation health, urban expansion, and surface temperature, highlighting the environmental impacts of urbanization in this region over the specified time frame. Cloud masking was applied, and the data was processed for spatial and temporal analysis. NDVI was calculated to determine the density and health of vegetation. Using the calculated NDVI

values, vegetation change maps for 2013 and 2024 were created, and the spatial distribution of green area losses was analyzed (Figure 3).

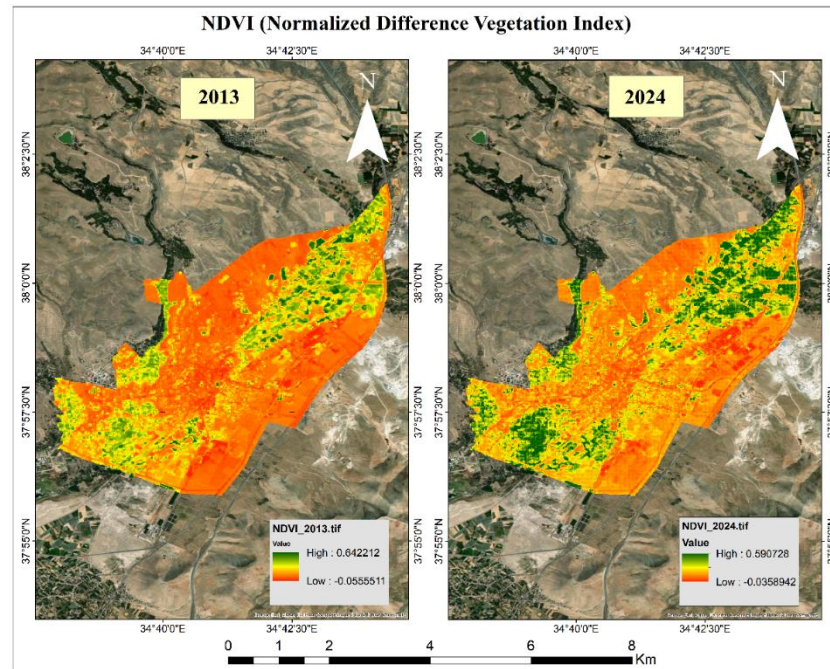


Figure 3. NDVI change map showing vegetation density variation from 2013 to 2024

NDBI is calculated to determine the urban density and build-out rate. The calculated NDBI values were used to determine the changes in urban growth and development rates. Between 2013 and 2024, the spatial distribution of housing growth was analyzed (Figure 4). The impact of construction on surface temperatures was assessed.

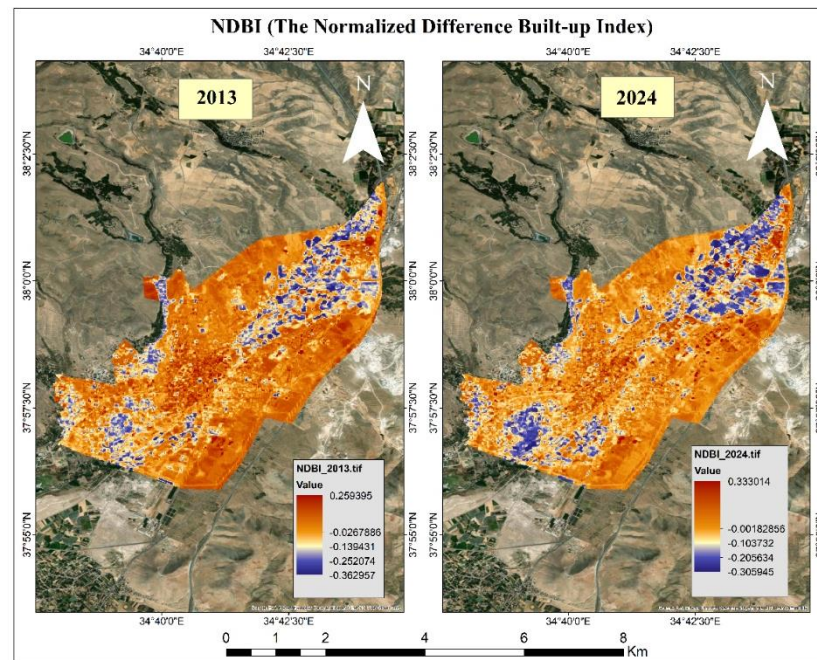


Figure 4. NDBI change map showing impervious surface expansion from 2013 to 2024

The chapter may be broken into subheadings. It should offer a short and precise su In the study, surface temperatures were also calculated using Landsat 8 TIRS Band 10. Three

basic steps were applied in the LST calculation process: conversion of DN values into radians, conversion of radians into brightness temperature, and conversion of brightness temperature into LST by applying emissivity correction. With the calculated LST values, the spatial distribution of the urban heat island effect was analyzed (Figure 5). Surface temperature changes between 2013 and 2024 were determined.

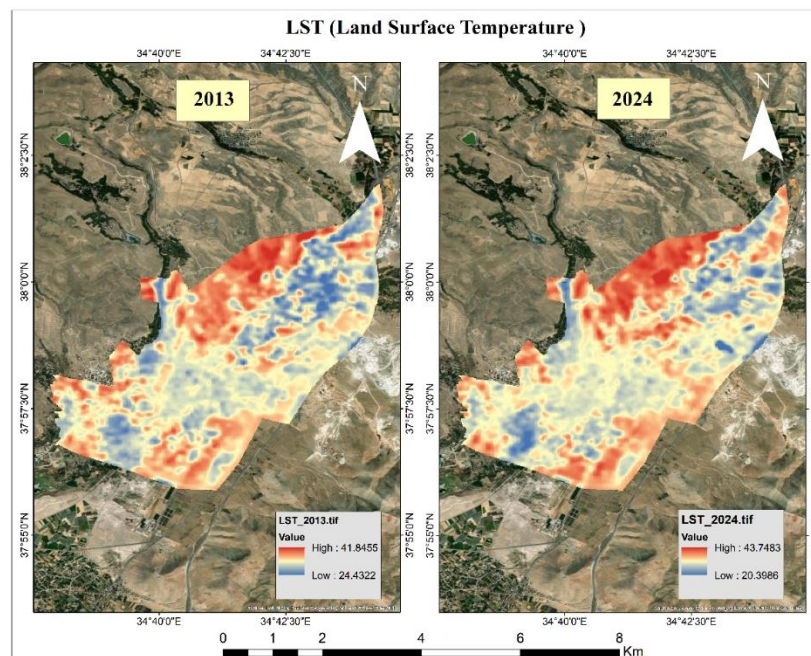


Figure 5. LST spatial distribution map (2013-2024)

In this study, the data of NDVI, NDBI, and LST indices for the years 2013 and 2024 were collected in similar geographical areas. The sample size for each index was determined as $n = 500$, and comparisons were made on the changes between both years. In order to evaluate the effects of environmental changes, especially urbanization and climate change, numerical values obtained from NDVI, NDBI, and LST indices were extracted from homogeneously distributed random points. In the ArcGIS 10.8 environment, 500 points were randomly generated within the study area.

NDVI, NDBI, and LST values of each point were extracted from the raster data with the “Extract to Values” tool. In this study, Table 2 presents the basic statistical properties of NDVI, NDBI, and LST indices for the years 2024 and 2013, and Table 2 was created to help us understand the distribution and characteristics of these indices.

Table 2. Basic statistics of NDVI, NDBI, and LST indices for the years 2024 and 2013

Descriptive	Indexes					
	NDVI_2024	NDVI_2013	NDBI_2024	NDBI_2013	LST_2024	LST_2013
Mean	0.18	0.18	-0.04	-0.05	35.01	33.40
Median	0.14	0.14	-0.01	-0.01	34.86	33.53
Variance	0.01	0.01	0.01	0.01	10.73	10.17
Std. Dev.	0.11	0.11	0.08	0.08	3.28	3.19
Minimum	0.00	0.00	-0.32	-0.41	0.00	0.00
Maximum	0.57	0.61	0.14	0.07	42.56	41.19
Range	0.57	0.61	0.46	0.48	42.56	41.19
Int. Range	0.15	0.14	0.10	0.10	2.98	3.17
Skewness	1.01	1.23	-1.08	-1.43	-4.74	-4.54
Kurtosis	0.21	0.98	0.67	1.90	50.88	46.69

In this table, NDVI values have remained largely constant between 2013 and 2024. The mean value remains unchanged at 0.18 and the median at 0.14, while the maximum value decreases from 0.61 in 2013 to 0.57 in 2024. This indicates that the overall vegetation density is largely maintained, but some areas may experience a decrease. On the other hand, NDBI values have increased at minimum and maximum levels. While the minimum value was -0.41 in 2013, it increased to -0.32 in 2024, while the maximum value increased from 0.07 to 0.14. This increase indicates that construction is expanding and urban areas are increasing. The most striking change is seen in LST data. The average surface temperature increased from 33.40°C in 2013 to 35.01°C in 2024, while the maximum temperature increased from 41.19°C to 42.56°C. This increase shows that surface temperatures are increasing, especially due to urbanization, and the urban heat island effect is getting stronger.

In addition, in this study, the conformity of NDVI, NDBI, and LST indices for the years 2013 and 2024 to normal distribution was examined using Kolmogorov-Smirnov and Shapiro-Wilk tests. Both tests are used to determine whether the data deviates from a normal distribution. Since normal distribution is the basic assumption in many statistical analyses, performing these tests is critical for the validity of modeling and analysis. Table 3 below presents the results of the Kolmogorov-Smirnov (K-S) and Shapiro-Wilk tests.

Table 3. Kolmogorov-Smirnov (K-S) and Shapiro-Wilk normal distribution test results

Indexes	Tests of Normality					
	Kolmogorov-Smirnov ^a			Shapiro-Wilk		
	Statistic	df	Sig.	Statistic	df	Sig.
NDVI_2024	0.152	500	0.000	0.898	500	0.000
NDVI_2013	0.157	500	0.000	0.879	500	0.000
NDBI_2024	0.150	500	0.000	0.903	500	0.000
NDBI_2013	0.157	500	0.000	0.862	500	0.000
LST_2024	0.124	500	0.000	0.715	500	0.000
LST_2013	0.087	500	0.000	0.739	500	0.000
a. Lilliefors Significance Correction						

In this table, the significance (Sig.) values for all indices in the Kolmogorov-Smirnov and Shapiro-Wilk tests were 0.000. Since $p < 0.05$ for all indices, the NDVI, NDBI, and LST values for the years 2013 and 2024 do not follow a normal distribution. This indicates that the data may be skewed or have many peaks. Especially the low Shapiro-Wilk statistic values of the LST data suggest that there is a greater skewness or outliers in the temperature distribution. Therefore, it would be more appropriate to use non-parametric tests (Mann-Whitney U, Wilcoxon Signed Rank, Kruskal-Wallis, etc.) instead of parametric tests in statistical analyses. In addition, different statistical graphs were drawn to visually present the distribution and normality analysis of the NDVI data for 2024 as an example to see whether the data are close to the normal distribution. 2024 NDVI data histogram, box plot, normal distribution plot, and normality plot without trend are given in Figure 6 below.

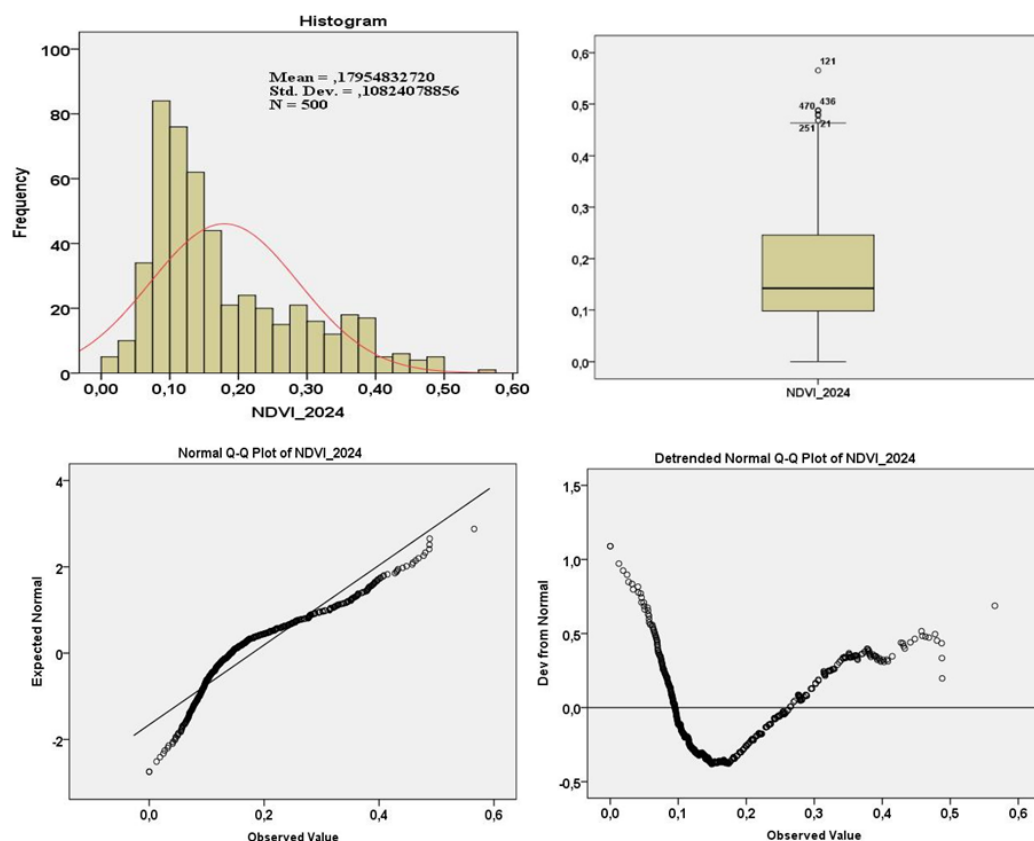


Figure 6. Normality analysis showing the distribution of NDVI data for 2024

The histogram plot in Figure 7 shows the skewness and distribution of the NDVI_2024 data, with most of the data concentrated around 0.1, exhibiting a left-skewed distribution. This indicates that most of the study area has low NDVI values, but some areas have dense vegetation. As the standard deviation (0.108) is low, the data are distributed close to the mean. The box plot visualizes the distribution and outliers. The median is close to the lower quartile, indicating that the data is asymmetrically distributed and skewed to the left. There are also some outliers around 0.5, indicating dense vegetation. In general, NDVI values are concentrated between 0.0 and 0.3. The normal scatter plot evaluates the conformity of the data to a normal distribution. Significant deviations are seen at low and high extremes, indicating that the data do not fit the normal distribution and exhibit a skewed distribution. Especially high outliers indicate areas with dense vegetation. The Trendless Normality plot shows in detail how much the data deviate from a normal distribution. At low and high values, the deviations are pronounced, while at intermediate values, the deviations are smaller. This indicates that the data generally deviate from a normal distribution and that there are significant deviations in extreme values.

Using parametric and nonparametric tests together in the analyses ensures that the most appropriate test is selected according to the characteristics of the data set and increases the reliability of the results. While parametric tests are based on certain assumptions, nonparametric tests give more robust results when these assumptions are not met. If the results of two tests confirm each other, the analysis becomes more reliable. While parametric tests provide more precise results, nonparametric tests are valid for a wider range of data. This approach provides a more comprehensive assessment for heterogeneous data sets or non-normal distributions. For this purpose, parametric and nonparametric tests were applied for the paired sample t-test and correlation analysis for NDVI, NDBI, and LST index values for the years 2024 and 2013. In this study, the relationships between NDVI, NDBI, and

LST variables for 2013 were analyzed by Pearson, Kendall's tau-b, and Spearman's rho correlation methods. The parametric (Pearson) and non-parametric (Kendall's tau-b and Spearman's rho) correlation coefficients in Table 4 below show the relationships between NDVI, NDBI, and LST variables in 2013 and 2024. Correlation coefficients (values ranging from -1 to 1) provide information about the direction and strength of the relationship between variables. Negative correlations indicate an inverse relationship, while positive correlations indicate a same-direction relationship. Furthermore, the correlations are statistically significant at the 0.01 significance level, indicating that the findings are reliable.

Table 4. Parametric (Pearson) and non-parametric (Kendall's tau-b and Spearman's rho) correlation coefficients

Correlations			2013			2024		
			NDVI	NDBI	LST	NDVI	NDBI	LST
Parametric	Pearson	NDV	1	-0,929	-0,372	1	-0,910	-0,320
		NDB	-0,929	1	0,432	-0,910	1	0,392
		LST	-0,372	0,432	1	-0,320	0,392	1
Nonparametric	Kendall's tau_b	NDV	1	-0,600	-0,334	1	-0,581	-0,325
		NDB	-0,600	1	0,368	-0,581	1	0,375
		LST	-0,334	0,368	1	-0,325	0,375	1
	Spearman's rho	NDV	1	-0,777	-0,466	1	-0,762	-0,461
		NDB	-0,777	1	0,518	-0,762	1	0,533
		LST	-0,466	0,518	1	-0,461	0,533	1
		Correlation is significant at the 0.01 level (2-tailed).						

As an example, in this table, according to the parametric Pearson correlation coefficients for 2013, there is a very strong negative correlation of -0.929 between NDVI and NDBI. This indicates that as vegetation cover increases, urbanization decreases (or vice versa). This result is naturally expected because as the urban area expands, green areas decrease. There is a negative correlation of -0.372 between NDVI and LST. This indicates that surface temperature decreases with increasing vegetation cover. Vegetation cover is an important factor in reducing surface temperature (e.g., due to evapotranspiration and shade effect). There is a positive correlation of 0.432 between NDBI and LST. This indicates that surface temperature increases with increasing urbanization. Artificial surfaces (concrete, asphalt, etc.) retain more heat than natural surfaces, increasing the urban heat island effect.

In general, all parametric and non-parametric correlation methods show similar trends. The strong negative correlation between NDVI and NDBI supports that urbanization causes a loss of green space. The negative correlation between NDVI and LST indicates that vegetation has a decreasing effect on surface temperature, while the positive correlation between NDBI and LST confirms that urbanization increases surface temperature. Although there are small differences between parametric and non-parametric methods, the general trend is the same. These findings show that in areas where urbanization increases, surface temperature increases, while vegetation cover decreases the temperature. The importance of protecting green areas should be emphasized during urbanization planning.

In addition, parametric paired sample t-tests and non-parametric Wilcoxon paired pairs tests were applied in this study to test whether the mean differences of NDVI, NDBI, and LST indices between 2024 and 2013 are significant. Table 5 below shows the results of the Paired Sample t-Test, and Table 6 shows the results of the Wilcoxon Matched Pairs Test.

Table 5. Paired Sample t-Test Results

Paired Differences	Mean	Std. Deviation	Std. Error Mean	95% Confidence Interval of the Difference		t	df	Sig. (2-tailed)
				Lower	Upper			
NDVI_2024/ 2013	0.00	0.07	0.00	-0.01	0.00	-0.72	499.00	0.47
NDBI_2024/2013	0.01	0.07	0.00	0.00	0.01	2.38	499.00	0.02
LST_2024/ 2013	1.62	1.70	0.08	1.47	1.76	21.32	499.00	0.00

Table 6. Wilcoxon Matched Pairs Test results

Test Statistics ^a			
	NDVI_2024/ NDVI_2013	NDBI_2024/ NDBI_2013	LST_2024/ LST_2013
Z	-1,837	-3,361	-16,446
Asymp. Sig. (2-tailed)	0.066	0.000	0.000
^a Wilcoxon Signed Ranks Test			

According to the paired sample t-test results in Table 6, the changes in NDVI, NDBI, and LST between 2013 and 2024 were analyzed. Since the mean difference for NDVI is 0.00 and the p-value is 0.47, it is concluded that there is no significant change. For NDBI, the mean difference is 0.01 and the p-value is 0.02, which is statistically significant, indicating that urbanization has increased. For LST, the mean difference is 1.62°C, and the p-value is 0.00, which is significant, indicating that there has been a significant increase in surface temperature, which may be related to factors such as urbanization. According to the Wilcoxon Matched Pairs Test results in Table 10, there is no significant difference in terms of NDVI, while significant differences are observed in NDBI and LST indices between 2024 and 2013. In general, although there is no significant change in vegetation cover between 2013 and 2024, urbanization has increased significantly, and as a result, a significant increase in surface temperatures has been observed. These findings are important in terms of showing the effects of urbanization on the ecosystem and the increase in the urban heat island effect.

In addition, optimal threshold values were determined by applying the Otsu thresholding method for each index between 2013 and 2024 for Niğde province. Masking was performed on the raster maps produced using NDVI and NDBI indices in line with the determined threshold values, and impervious surfaces were created. In Figure 7, impervious surfaces (urban areas, roads, buildings, etc.) are shown in red, and other surfaces are shown in black. Thanks to this method, the spatial change between 2013 and 2024 is made more evident, and the related spatial changes are detailed in Table 7.

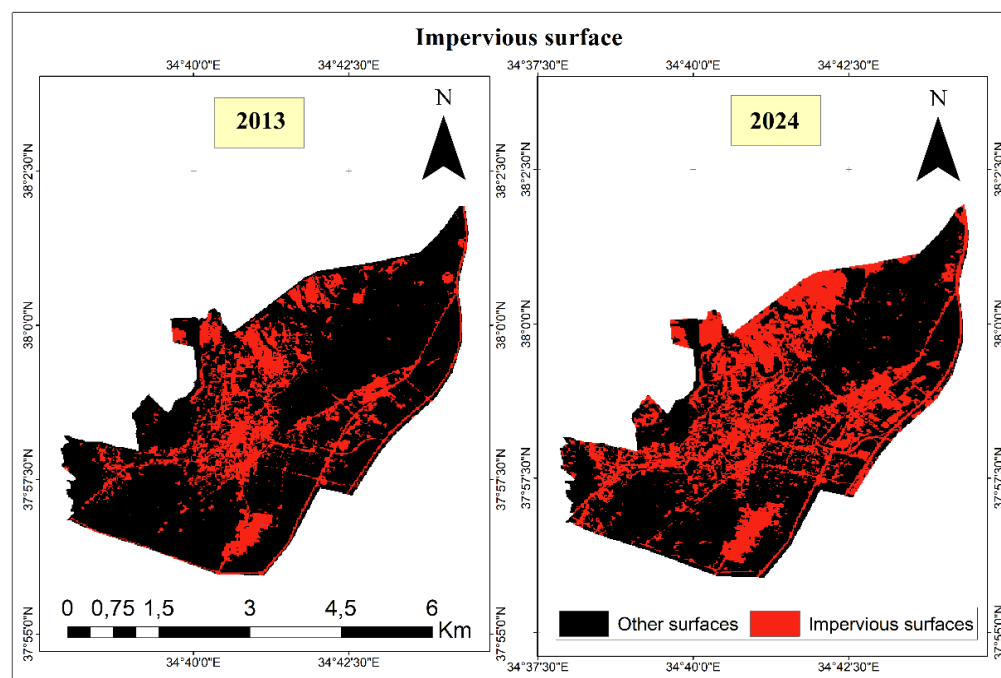


Figure 7. Spatial distribution and temporal change detection of impervious surfaces in the city center

Table 7. Quantitative assessment of impervious surface area changes between 2013 and 2024

Year	Impervious surface (km ²)	Difference area (+/-)	Percentage change (+/-)	Other Surface (km ²)	Difference area (+/-)	Percentage change (+/-)	Total Surface Area (km ²)
2013	14.02	8.36	% 59.63	51.82	-8.36	% -16.13	65.84
2024	22.38			43.46			65.84

When the impervious surface change between 2013 and 2024 is examined in Figure 7, it is determined that a significant increase has occurred in Niğde city center. According to Table 7, the impervious surface area, which was 14.02 km² in 2013, increased to 22.38 km² in 2024, which corresponds to an expansion of 59.63%. Correspondingly, the area of other surfaces decreased from 51.82 km² to 43.46 km², a decrease of 8.36 km². The expansion of impervious surfaces had a major impact on agricultural areas, with many agricultural areas being converted into urban areas. This situation shows that urbanization is progressing in a way to cover the surrounding natural and agricultural areas and that spatial expansion is concentrated in certain directions.

Spatial analysis reveals that the increase in impervious surfaces is especially concentrated in the southwest, east, and southeast directions of the city center. The increase in new constructions around the industrial zone and the university in the southwest direction and the expansion of industrial facilities have contributed to the increase in impervious surfaces in these regions. In the eastern and southeastern directions, expansion was observed towards the Kayseri road network, and the development of transportation infrastructure and the formation of new residential areas in these regions are among the important factors. It is observed that a significant portion of the agricultural areas around the city center have been transformed into impermeable surfaces, which has led to a decrease in agricultural activities under the pressure of urbanization.

LST maps also reveal the relationship between the increase in impervious surfaces and surface temperatures. When the 2013 and 2024 LST maps are compared, it is observed that the temperature values increase, especially in the regions where impervious surfaces are dense. In 2013, the highest surface temperature was 41.84°C, while this value increased to

43.74°C in 2024. However, while the lowest surface temperature was 24.43°C in 2013, it decreased to 20.39°C in 2024. This shows that the urban heat island effect becomes more pronounced over time and is directly related to the increase in impervious surfaces. In particular, temperatures increase more in the industrial zone, around the university, and along the Kayseri road network. This increase can be explained by the fact that impervious surfaces absorb sunlight and retain more heat, and the cooling effect is weakened due to the decrease in natural surfaces. In this process, the protection of green areas and the development of balanced land use policies are of great importance. Likewise, the areal change in vegetation density between 2013 and 2024 is given in Table 8. Vegetation density was analyzed in 5 classes (Aquino et al. 2018).

Table 8. Quantitative assessment of vegetation density changes between 2013 and 2024

Year	Bare soil and/or water (km ²)	Very low (km ²)	Low (km ²)	Moderately Low (km ²)	Moderately High (km ²)	High (km ²)
2013	0.013	16.28	37.23	11.34	0.98	49.55
2024	0.011	16.30	38.08	10.97	0.49	49.54

Between 2013 and 2024, despite the significant increase in impervious surfaces in Niğde city center, the size of the areas with high-density vegetation cover remained almost constant from 49.55 km² in 2013 to 49.54 km² in 2024. This is an indication of the importance that Niğde Municipality attaches to green space arrangements, especially from 2022 onwards. In 2022, the Niğde Municipality Parks and Gardens Directorate constructed new parks and renovated existing parks in different parts of the city. In addition, 25,000 m² of Gebere Dam Recreation Area was turfed with the hydroseeding method, and a large area of 600,000 m² was greened with regular plant maintenance. Table 8 shows that the area of dense vegetation decreased by 50% from 0.98 km² in 2013 to 0.49 km² in 2024. The area of medium-dense vegetation decreased slightly from 11.34 km² in 2013 to 10.97 km² in 2024 (-0.37 km²). The sparse vegetation area increased from 37.23 km² in 2013 to 38.08 km² in 2024, an increase of 0.85 km². There is a minimal increase of 0.02 km² in the area of very low-density vegetation in 2024 compared to 2013. The land group indicating the presence of water surface or bare land showed a slight decrease from 0.013 km² to 0.011 km². Between 2013 and 2024, although the total vegetation area remained largely unchanged, significant differences were observed in the density distribution of vegetation. The area of dense vegetation decreased by 50%, while the area of sparse vegetation increased. This means that the dense vegetation has been destroyed and transformed into a sparser vegetation structure. Medium-density vegetation also showed a slight decrease, while the area of bare land increased slightly. These changes can be attributed to factors such as urban expansion, agricultural activities, land use changes, and climatic influences.

4. Discussion

In this study, changes in urban growth, impervious surface increase, and surface temperatures in Niğde city center between 2013 and 2024 were analyzed with remote sensing data. The findings show that there is a strong positive correlation, especially between NDBI and LST. This is in line with the findings of Guha et al. (2021) and Chen et al. (2013). Both studies revealed that LST values increase with the increase in construction in different geographical areas and emphasized that this relationship is more pronounced, especially in summer months. In Niğde city center, it was observed that the urban heat island (UHI) effect increased spatially with the intensification of construction, especially in areas such as industrial zones, transportation axes, and around the university. This situation was also observed in the studies conducted by Keerthi Naidu & Chundeli (2023) in Bengaluru, India.

In these studies, it was stated that LULC changes have significant effects on LST, and this effect can be detailed with spatial analysis.

On the other hand, no statistically significant change in the NDVI index was observed in our study. This finding contradicts the results obtained in different regional studies. For example, Alademomi et al. (2022) reported a significant decrease in NDVI values in the Lagos metropolitan area between 2002 and 2019, while LST increased in parallel. Similarly, Keerthi Keerthi Naidu & Chundeli (2023) emphasize that there was a loss of over 50% in NDVI in Bengaluru city between 2003 and 2021, which is directly related to the increasing construction.

Previous studies in Niğde also reveal that urbanization has a significant impact on land use patterns. Kızılelma et al. (2013), in a study based on satellite imagery, found that the urban area of Niğde grew approximately 2.5 times between 1984 and 2011, with an average annual growth rate of 6%. Especially in the 2000-2011 period, with a growth rate of 11.7%, sparse vegetation and dry agricultural lands were transformed into residential areas. This study emphasizes that urban centers of attraction such as universities, organized industrial zones, and TOKI are effective in determining the direction of urbanization. In this context, it is seen that the increases in LST and impervious surface concentration identified in the current study are spatially coincident with these expansion trends. In addition, the results of the LULC analysis conducted in and around the center of Niğde reported that the replacement of agricultural areas by residential areas put pressure on plant density. These results contradict our current study. However, it is thought that this difference can be explained by the green space, park, and afforestation projects implemented by Niğde Municipality after 2022. These projects ensured the preservation of dense vegetation cover and the addition of new green areas, especially in areas with dense construction, thus preventing a significant decrease in overall NDVI values. This demonstrates the impact of local government interventions on environmental indicators and helps explain regional differences in the literature.

In addition, normality and t-test analyses show that the changes in the NDBI and LST indices evaluated in the study are statistically significant and directional. This shows that the environmental impacts of the urbanization process are systematic rather than random and necessitates long-term monitoring.

Conclusions

This study performed a statistical and spatial analysis of the relationship between urban growth, impervious surface increase, and surface temperatures between 2013 and 2024 in Niğde city center. The analysis using remote sensing data and statistical tests revealed that urbanization has put significant pressure on natural surfaces and the urban heat island effect has become increasingly evident. In particular, a strong positive correlation was found between NDBI and LST indices, confirming that surface temperatures increase with increasing urbanization. Paired sample t-test results show that there is no significant change in the NDVI index, but there are statistically significant differences in the NDBI and LST indices. Normal distribution tests also revealed that the variation of the indices over time was not random and followed a clear trend.

The results obtained in the study show that surface temperatures increased in areas with dense construction, whereas the temperature increase was more limited in areas with relatively protected vegetation. The fact that no significant change was observed in the NDVI index indicates the protective effect of afforestation and green area projects carried out in previous years on vegetation cover. This finding contradicts some studies in the existing literature and shows that spatial interventions at the local level enable differentiation on environmental indicators.

The findings of the study show that natural areas especially agricultural lands have been transformed into settlements due to the increase in impervious surfaces. Especially around industrial zones, transportation lines, and university, construction has accelerated, and this situation reveals that the urban heat island effect has intensified regionally. LST analyses confirm that surface temperatures have increased significantly in these regions. However, in recent years, green infrastructure projects carried out by Niğde Municipality have contributed to the preservation of vegetation cover, mitigating the urban heat island effect in some areas. These local interventions reveal the decisive role of city-level spatial planning on environmental impacts.

The findings show that the environmental impacts of the urbanization process are not limited to physical space but also affect climatic and ecological processes. Remote sensing and geographical information systems-based analyses are considered to play a critical role in quantitatively monitoring such changes and providing a scientific basis for spatial decision-making processes.

In line with these findings, some policy recommendations can be made to make urban development sustainable. First of all, spatial planning decisions should be taken to protect agricultural areas and natural surfaces in the urbanization process. To offset the increase in impervious surfaces, nature-based solutions such as increasing urban green spaces, integrating rainwater management systems, and using permeable surfaces should be encouraged. Municipal and local governments should support sustainable land management by expanding green space projects within the city. In addition, remote sensing and geographic information systems-based analyses should be conducted regularly to monitor the environmental impacts of urbanization, and these data should be used effectively in decision-making processes.

As a result of the study, it was determined that increasing impervious surfaces and decreasing natural areas in Niğde city center directly affect the increase in urban temperature. Therefore, integrated planning strategies should be developed to minimize the environmental impacts of the urbanization process. The expansion of green infrastructure projects is critical for sustainable urban development. Remote sensing techniques should be considered as an important tool for monitoring such environmental changes and developing sustainable development policies. Although the study was conducted at the scale of Niğde city center, it can also provide a basis for comparative analysis for medium-sized cities with similar urban dynamics.

Acknowledgments: The authors would like to thank the United States Geological Survey (USGS) for providing open access to satellite data. We also express our gratitude to the developers and maintainers of the Google Earth Engine (GEE) platform for enabling open-access geospatial analysis.

Author Contributions:

M. G. Gümüş: Conceptualization, Literature review, Designed the research methodology, Spatial analyzed, Writing—original draft preparation.

K. Gümüş: Statistic analyzed, Data curation, Writing-reviewing and editing.

Research and publication ethics statement: In the study, the authors declare that there is no violation of research and publication ethics and that the study does not require ethics committee approval.

Conflicts of Interest: The authors declare no conflicts of interest.

References

- Akyürek, Ö. (2020). Determination of Land Surface Temperature with thermal remote sensing images: A case study Kocaeli province. *Journal of Natural Hazards and Environment*, 6(2), 377-390. <https://doi.org/10.21324/dacd.667594>
- Alademomi, A. S., Okolie, C. J., Daramola, O. E., Akinnusi, S. A., Adediran, E., Olanrewaju, H. O., Alabi, A. O., Salami, T. J., & Odumosu, J. (2022). The interrelationship between LST, NDVI, NDBI, and land cover change in a section of Lagos metropolis, Nigeria. *Applied Geomatics*, 14(2), 299-314. <https://doi.org/10.1007/s12518-022-00434-2>

- Aquino, D. D. N., Rocha Neto, O. C. D., Moreira, M. A., Teixeira, A. D. S., & Andrade, E. M. D. (2018). Use of remote sensing to identify areas at risk of degradation in the semi-arid region. *Revista Ciência Agronômica*, 49, pp. 420–429. <https://doi.org/10.5935/1806-6690.20180047>
- Bauer, M. E., Heinert, N. J., Doyle, J. K., & Yuan, F. (2004). Impervious surface mapping and change monitoring using Landsat remote sensing. *Proceedings Book of ASPRS Annual Conference Proceedings: American Society for Photogrammetry and Remote Sensing* Bethesda, MD, USA.
- Blair, R. C., & Higgins, J. J. (1985). Comparison of the power of the paired samples t test to that of Wilcoxon's signed-ranks test under various population shapes. *Psychological Bulletin*, 97(1), 119. <https://doi.org/10.1037/0033-2909.97.1.119>
- Chen, L., Li, M., Huang, F., & Xu, S. (2013, December 16-18). Relationships of LST to NDBI and NDVI in Wuhan City based on Landsat ETM+ image [Paper presentation]. 6th international congress on image and signal processing (CISP), Hangzhou, China. <https://doi.org/10.1109/CISP.2013.6745282>
- Chen, Y., Wang, J., & Li, X. (2002). A study on urban thermal field in summer based on satellite remote sensing. *Remote Sensing for Land and Resources*, 4(1), 55–59.
- Fıçıcı, M. (2024). Analysis of urban sprawl along the coastline of Trabzon province between 1980-2030 using GHSL (global human settlement layer) and GEE (google earth engine). *Journal of Anatolian Geography*, 2(2), 97–107.
- Genceli, M. (2007). Kolmogorov-smirnov, lilliefors and shapiro-wilk tests for normality. *Sigma Journal of Engineering and Natural Sciences*, 25(4), 306–328.
- Gorelick, N. (2013, April). Google earth engine. *Proceedings Book of EGU General Assembly Conference*. Vienna, Austria.
- Guha, S., Govil, H., Gill, N., & Dey, A. (2021). A long-term seasonal analysis on the relationship between LST and NDBI using Landsat data. *Quaternary International*, 575, 249–258. <https://doi.org/10.1016/j.quaint.2020.06.041>
- Gümüş, M. G. (2024). Forecasting future scenarios of coastline changes in Türkiye's Seyhan Basin: a comparative analysis of statistical methods and Kalman Filtering (2033–2043). *Earth Science Informatics*, 17, 5207–5232. <https://doi.org/10.1007/s12145-024-01445-w>
- Gümüş, M. G., & Durduran, S. S. (2023). Satellite-based investigation of drought effect on vegetation health index: Beyşehir-Kaşaklı Sub-Basin, Turkey. *Bulletin of Geophysics & Oceanography*, 64(1), 89–112. <https://doi.org/10.4430/bgo00403>
- Gümüş, M. G., & Durduran, S. S. (2024). Determination of Potential Geothermal Areas in Konya Seydişehir District Using GIS-based Multi-Criteria Decision Analysis. *Turkish Journal of Remote Sensing*, 6(1), 26–34. <https://doi.org/10.51489/tuzal.1400620>
- Hatfield, J. L., Kanemasu, E. T., Asrar, G., Jackson, R. D., Pinter Jr, P. J., Reginato, R. J., & Idso, S. B. (1985). Leaf-area estimates from spectral measurements over various planting dates of wheat. *International Journal of Remote Sensing*, 6(1), 167–175. <https://doi.org/10.1080/01431168508948432>
- İnan, M. (2009). The spectral relationships between remote sensing data and dendrometric parameters of forest stand. *Journal of Engineering and Architecture Faculty of Eskişehir Osmangazi University*, 22(3), 21–33.
- Jamei, Y., Seyedmahmoudian, M., Jamei, E., Horan, B., Mekhilef, S., & Stojcevski, A. (2022). Investigating the relationship between land use/land cover change and land surface temperature using Google Earth engine; case study: Melbourne, Australia. *Sustainability*, 14(22), 14868. <https://doi.org/10.3390/su142214868>
- Kale, M. M., & Erişmiş, M. (2024). Analysis of the spatial changes in lake Eğirdir using remote sensing and geographic information systems. *International Journal of Geography and Geography Education*, (52), 122–140. <https://doi.org/10.32003/igge.1380588>
- Keerthi Naidu, B. N., & Chundeli, F. A. (2023). Assessing LULC changes and LST through NDVI and NDBI spatial indicators: A case of Bengaluru, India. *GeoJournal*, 88(4), 4335–4350. <https://doi.org/10.1007/s10708-023-10862-1>
- Kesikoğlu, M. H., Ozkan, C., & Kaynak, T. (2021). The impact of impervious surface, vegetation, and soil areas on land surface temperatures in a semi-arid region using Landsat satellite images enriched with Ndaishi method data. *Environmental Monitoring and Assessment*, 193, 143. <https://doi.org/10.1007/s10661-021-08916-3>
- Kılıç, A. F. (2022). The effect of categories and distribution of variables on correlation coefficients. *Ege Journal of Education*, 23(1), 50–80. <https://doi.org/10.12984/egeefd.890104>
- Kızılelma, Y., Karabulut, M., Gürbüz, M., Topuz, M., & Ceylan, E. (2013). Niğde şehri ve yakın çevresinin zamansal değişiminin uzaktan algılama ve CBS kullanılarak incelenmesi. *Zeitschrift für die Welt der Türken-Journal of World of Turks*, 5(3), 21–34.
- KTB. (2014). Geographical characteristics of Niğde. Retrieved January 11, 2025, from <https://nigde.ktb.gov.tr/Eklenti/33622%2Cnigde-nin-cografi-ozellikleri.pdf?0=>
- Lambin, E. F., & Ehrlich, D. (1996). The surface temperature-vegetation index space for land cover and land-cover change analysis. *International Journal of Remote Sensing*, 17(3), 463–487. <https://doi.org/10.1080/01431169608949021>
- Liu, J., Li, Y., Zhang, Y., & Liu, X. (2023). Large-scale impervious surface area mapping and pattern evolution of the Yellow river delta using Sentinel-1/2 on the GEE. *Remote Sensing*, 15(1), 136. <https://doi.org/10.3390/rs15010136>
- Manfei, X., Fralick, D., Zheng, J. Z., Wang, B., Xin, M. T. U., & Changyong, F. (2017). The differences and similarities between two-sample t-test and paired t-test. *Shanghai Archives of Psychiatry*, 29(3), 184. <https://doi.org/10.11919/j.issn.1002-0829.217070>

- Okoye, K., & Hosseini, S. (2024). T-test statistics in R: Independent samples, paired sample, and one sample T-tests. In: R programming: statistical data analysis in research. Springer. https://doi.org/10.1007/978-981-97-3385-9_8
- Parekh, J. R., Poortinga, A., Bhandari, B., Mayer, T., Saah, D., & Chishtie, F. (2021). Automatic detection of impervious surfaces from remotely sensed data using deep learning. *Remote Sensing*, 13(16), 3166. <https://doi.org/10.3390/rs13163166>
- Razali, N. M., & Wah, Y. B. (2011). Power comparisons of shapiro-wilk, kolmogorov-smirnov, lilliefors and anderson-darling tests. *Journal of Statistical Modeling and Analytics*, 2(1), 21–33.
- Sarkar Chaudhuri, A., Singh, P., & Rai, S. C. (2017). Assessment of impervious surface growth in urban environment through remote sensing estimates. *Environmental Earth Sciences*, 76, 1–14. <https://doi.org/10.1007/s12665-017-6877-1>
- Shrestha, B., Ahmad, S., & Stephen, H. (2021). Fusion of Sentinel-1 and Sentinel-2 data in mapping the impervious surfaces at city scale. *Environmental Monitoring and Assessment*, 193(9), 556. <https://doi.org/10.1007/s10661-021-09321-6>
- Sobrino, J. A., & Raissouni, N. (2000). Toward remote sensing methods for land cover dynamic monitoring: application to Morocco. *International Journal of Remote Sensing*, 21, 353–366. <https://doi.org/10.1080/014311600210876>
- Tonyaloğlu, E. E. (2019). The evaluation of the impact of urbanisation on urban thermal environment in the case of Aydin. *Turkish Journal of Landscape Research*, 2(1), 1–13.
- TÜİK. (2025). Provincial Populations by Year. Retrieved January 11, 2025, from <https://data.tuik.gov.tr/Bulten/Index?p=Adrese-Dayali-Nufus-Kayit-Sistemi-Sonuclari-2024-53783>
- UNPD. (2015). World Urbanization Prospects: The 2014 Revision. Retrieved December 22, 2024, from <https://www.un.org/development/desa/pd/>
- Ünver, A., & Başkaya, Z. (2024). Building density change analysis with NDVI, NDBI and UI Analyzes (1999-2022): Yıldırım District (Bursa) example. *Journal of Geography*, (49), pp. 65–81. <https://doi.org/10.26650/JGEOG2024-1441862>
- USGS. (2013). Landsat missions (Landsat 8). Retrieved December 02, 2024, from <https://www.usgs.gov/landsat-missions/landsat-8>
- Voogt, J. A., & Oke, T. R. (2003). Thermal remote sensing of urban climates. *Remote Sensing of Environment*, 86(3), 370–384. [https://doi.org/10.1016/S0034-4257\(03\)00079-8](https://doi.org/10.1016/S0034-4257(03)00079-8)
- Weng, Q., Lu, D., & Schubring, J. (2004). Estimation of land surface temperature–vegetation abundance relationship for urban heat island studies. *Remote Sensing of Environment*, 89(4), 467–483. <https://doi.org/10.1016/j.rse.2003.11.005>
- Yuan, F., & Bauer, M. E. (2007). Comparison of impervious surface area and normalized difference vegetation index as indicators of surface urban heat island effects in Landsat imagery. *Remote Sensing of Environment*, 106(3), 375–386. <https://doi.org/10.1016/j.rse.2006.09.003>
- Zhang, Y., Odeh, I. O., & Han, C. (2009). Bi-temporal characterization of land surface temperature in relation to impervious surface area, NDVI and NDBI, using a sub-pixel image analysis. *International Journal of Applied Earth Observation and Geoinformation*, 11(4), pp.256-264. <https://doi.org/10.1016/j.jag.2009.03.001>

Appendix A

```
area = ee.FeatureCollection("Nigde");
var image = ee.ImageCollection("LANDSAT/LC08/C02/T1")
    .filterDate('2018-03-01', '2023-06-31')
    .filter('CLOUD_COVER < 5')
    .filterBounds(area)
var clip=image.mean().clip(area)
//1.TOA Calc
//TOA = 0,0003342 * "Bant 10" + 0,1
var toa = clip.expression( '0.0003342*BAND10+0.1', { 'BAND10': clip.select('B10'), }).rename("TOA")
print(toa)
//2.BT Calc
//BT = (1321.0789 / Ln ((774.8853 /TOA) + 1)) - 273.15
var bt=toa.expression( '(1321.0789/log((774.8853/TOA)+1))-273.15',{ 'TOA':toa.select("TOA") }).rename('BT');
print(bt)
//3.NDVI
var nirBand = 'B5';
var redBand = 'B4';
var ndvi = clip.normalizedDifference([nirBand, redBand]).rename('NDVI');
var min = ee.Number(ndvi.reduceRegion({
    reducer: ee.Reducer.min(),
    geometry: area,
    scale: 30,
    maxPixels: 1e10
}).values().get(0));
var max = ee.Number(ndvi.reduceRegion({
```

```
reducer: ee.Reducer.max(),
geometry: area,
scale: 30,
maxPixels: 1e10
}).values().get(0));
print(min)
print(max)
//4.PV Calc
//Pv = Kare ((NDVI - NDVI min ) / (NDVI maks - NDVI min ))
var pv = (ndvi.subtract(min).divide(max.subtract(min))).pow(ee.Number(2))
//5.Emistivite Calc
//ε = 0,004 * P v + 0,986
var a=ee.Number(0.004)
var b=ee.Number(0.986)
var em=pv.multiply(a).add(b).rename('EMM')
//6.LST Calc
//LST = (BT / (1 + (0,00115 * BT / 1,4388) * Ln(ε)))
var termal= clip.select('B10').multiply(0.1)
var LST=bt.expression(
'(BT/(1+(0.00115*BT/1.4388)*log(e)))',{
'BT':bt.select('BT'),
'e':em.select('EMM'),
}).rename('LST')
var bandMap = {
nir : clip.select("B5"),
swir1 : clip.select("B6")};
var ndbi = clip.expression('(swir1 - nir) / (swir1 + nir)', bandMap).rename('NDBI');
```